A neural circuit for competing approach and defense underlying prey capture

Daniel Rossier[a], Violetta La Franca[a,b], Taddeo Salemi[a,c], Silvia Natale[a,d], and Cornelius T. Gross[a,1]

[a]Epigenetics and Neurobiology Unit, European Molecular Biology Laboratory, 00015 Monterotondo (RM), Italy; [b]Neurobiology Master's Program, Sapienza University of Rome, 00185 Rome, Italy; [c]Department of Biochemistry and Biophysics, Stockholm University, 10691 Stockholm, Sweden; and [d]Division of Pharmacology, Department of Neuroscience, Reproductive and Odontostomatologic Sciences, School of Medicine, University of Naples Federico II, 80131 Naples, Italy

Edited by Michael S. Fanselow, University of California, Los Angeles, CA, and accepted by Editorial Board Member Peter L. Strick February 11, 2021 (received for review July 22, 2020)

Predators must frequently balance competing approach and defensive behaviors elicited by a moving and potentially dangerous prey. Several brain circuits supporting predation have recently been localized. However, the mechanisms by which these circuits balance the conflict between approach and defense responses remain unknown. Laboratory mice initially show alternating approach and defense responses toward cockroaches, a natural prey, but with repeated exposure become avid hunters. Here, we used in vivo neural activity recording and cell-type specific manipulations in hunting male mice to identify neurons in the lateral hypothalamus and periaqueductal gray that encode and control predatory approach and defense behaviors. We found a subset of GABAergic neurons in lateral hypothalamus that specifically encoded hunting behaviors and whose stimulation triggered predation but not feeding. This population projects to the periaqueductal gray, and stimulation of these projections promoted predation. Neurons in periaqueductal gray encoded both approach and defensive behaviors but only initially when the mouse showed high levels of fear of the prey. Our findings allow us to propose that GABAergic neurons in lateral hypothalamus facilitate predation in part by suppressing defensive responses to prey encoded in the periaqueductal gray. Our results reveal a neural circuit mechanism for controlling the balance between conflicting approach and defensive behaviors elicited by the same stimulus.

PAG | LHA | aggression

The ability to seek and capture prey adeptly is a conserved behavior essential to the survival of numerous animal species. However, attacking prey brings risks for the predator, and efficient hunting requires a skillful balance between responding to threatening and appetitive prey cues. The neural circuits involved in this balance are unknown. Rodents naturally hunt and consume a variety of insects, and hunting behavior has been studied in the laboratory using rats given cockroaches or mice (1) and, more recently, in laboratory mice given crickets (2–5). In early studies, immediate early gene mapping during hunting identified the recruitment of lateral hypothalamus (LHA) (1, 6, 7) and periaqueductal gray (PAG) (7, 8), and electrical stimulation of either LHA (9–12) or PAG (13, 14) could initiate avid predatory attacks in rats and cats, suggesting the presence of neuronal cell populations that promote hunting in both these brain structures.

LHA has been historically regarded as a central node in the neural system controlling seeking behaviors, including feeding and predatory hunting (14–16). Recent circuit neuroscience work has confirmed this role by finding that stimulation of *Vgat*+ GABAergic neurons in LHA can trigger predation as well as feeding (5, 17–20). However, the role of these neurons in predation may be indirect, as any manipulation that increases food seeking is expected to promote motivation to hunt as well. Moreover, some studies in which LHA GABAergic neurons were optogenetically stimulated did not observe the full repertoire of feeding behaviors but instead found increased chewing activity, digging, or general motor activity (21–23), suggesting that the link between LHA-driven feeding and hunting may be more complex. One possible confound in these studies is their use of two different Cre driver lines (*Vgat*::Cre versus *Gad2*::Cre) that have been shown to target distinct LHA GABAergic neurons (23). Thus, it remains unclear to what extent different populations of LHA GABAergic neurons specifically encode and control predatory behaviors.

A link between LHA and PAG in predation was made by a recent study showing that activation of LHA to PAG projections can promote predatory hunting in mice (5), and the central importance of the PAG in hunting is further strengthened by several studies identifying a series of PAG afferents arising from different brain structures—including the central nucleus of the amygdala, medial preoptic area, and zona incerta—that promote predation (3, 4, 24, 25). However, the precise functional role of the PAG in hunting remains unclear. For example, it was found that inhibition of glutamatergic neurons in the lateral and ventrolateral PAG (l/vlPAG) by GABAergic inputs from the central nucleus of the amygdala promotes predatory behavior (3), suggesting that PAG neurons might function to suppress rather than promote predation. At the same time, other studies have shown that activation of glutamatergic neurons in l/vlPAG induces defensive behaviors (26), a finding that is consistent with an extensive literature linking PAG to both innate and learned defensive behavior (27–29). One explanation for these observations is that PAG has an antagonistic role in hunting by promoting defensive

Significance

Predatory hunting involves measured risk taking by the predator to anticipate dangerous defensive behavior from prey. This involves a mechanism where the motivation to hunt can overcome defensive behaviors toward prey to unlock attack. Here, we found that activation of a subset of GABAergic neurons in the lateral hypothalamus (LHA) promotes hunting but not feeding behavior. Stimulation of projections of these neurons to the periaqueductal gray (PAG), an area known to trigger defensive behaviors, decreased avoidance of prey. Single neuron recording during exposure to prey revealed two distinct PAG neuronal populations encoding risk assessment and flight. We conclude that in male mice, LHA GABAergic neurons are involved in blocking defensive behavior encoded in the PAG to overcome fear of prey.

Author contributions: D.R. and C.T.G. designed research; D.R., V.L.F., T.S., and S.N. performed research; D.R., V.L.F., T.S., S.N., and C.T.G. analyzed data; and D.R. and C.T.G. wrote the paper.

The authors declare no competing interest.

This article is a PNAS Direct Submission. M.S.F. is a guest editor invited by the Editorial Board.

[1]To whom correspondence may be addressed. Email: gross@embl.it.

This article contains supporting information online at https://www.pnas.org/lookup/suppl/doi:10.1073/pnas.2013411118/-/DCSupplemental.

Published April 5, 2021.

behaviors toward prey early in the encounter when familiarity with the prey is low. Suppression of these defensive responses by GABAergic inputs would therefore facilitate unimpeded predation.

Here, we identify *Gad2*+ neurons in LHA as those specifically recruited during predatory chasing and attack, and both are sufficient and necessary to drive hunting, but not feeding or social behavior, in male mice. Activation of LHA *Gad2*+ neuron projections to PAG decreased defensive responses to prey and promoted hunting during the early phases of predation when male mice learned to hunt cockroaches. Finally, in vivo calcium endoscopy identified a neural population in PAG that encoded risk assessment and flight behaviors elicited by prey. Notably, we failed to detect PAG neurons responsive to predatory pursuit or attack. These results point to a circuit in which activity in LHA *Gad2*+ neurons promotes hunting in part by suppressing defensive responses encoded in PAG.

Results

Mice Learn to Efficiently Hunt Cockroaches. To understand the contribution of the lateral hypothalamic seeking system to hunting behavior, we studied mice pursuing, capturing, and consuming cockroaches, a natural prey. Exposure of naïve mice to cockroaches elicited repeated attempts to approach and attack the prey interspersed with robust flight and freezing responses (Fig. 1*A* and Movie S1). Repeated exposure of mice to cockroaches led to a gradual decrease in defensive responses and latency to pursue and capture prey (Fig. 1 *A*–*E*), suggesting that either their fear of the prey diminishes or their motivation to hunt is increased with repeated exposure. In trained animals, hunting was typically initiated in 43 ± 11 s after the introduction of the prey compared to 391 ± 109 s in untrained animals. A predatory sequence usually involved bouts of pursuit and attack using mouth and forepaws followed by attempts to consume the immobilized prey. Residual movement of the immobilized prey during feeding occasionally interrupted the engagement and led to the initiation of new hunting bouts. Importantly, mice fed laboratory chow ad libitum showed robust predatory hunting behavior, arguing for a strong hunger-independent motivation for mice to pursue and capture prey. No difference in the gradual decrease in latency or increase in intensity of hunting behaviors was seen between male and female mice (*SI Appendix*, Fig. S1 *A*–*D*). The alternation between defensive and predatory behavior toward the cockroach

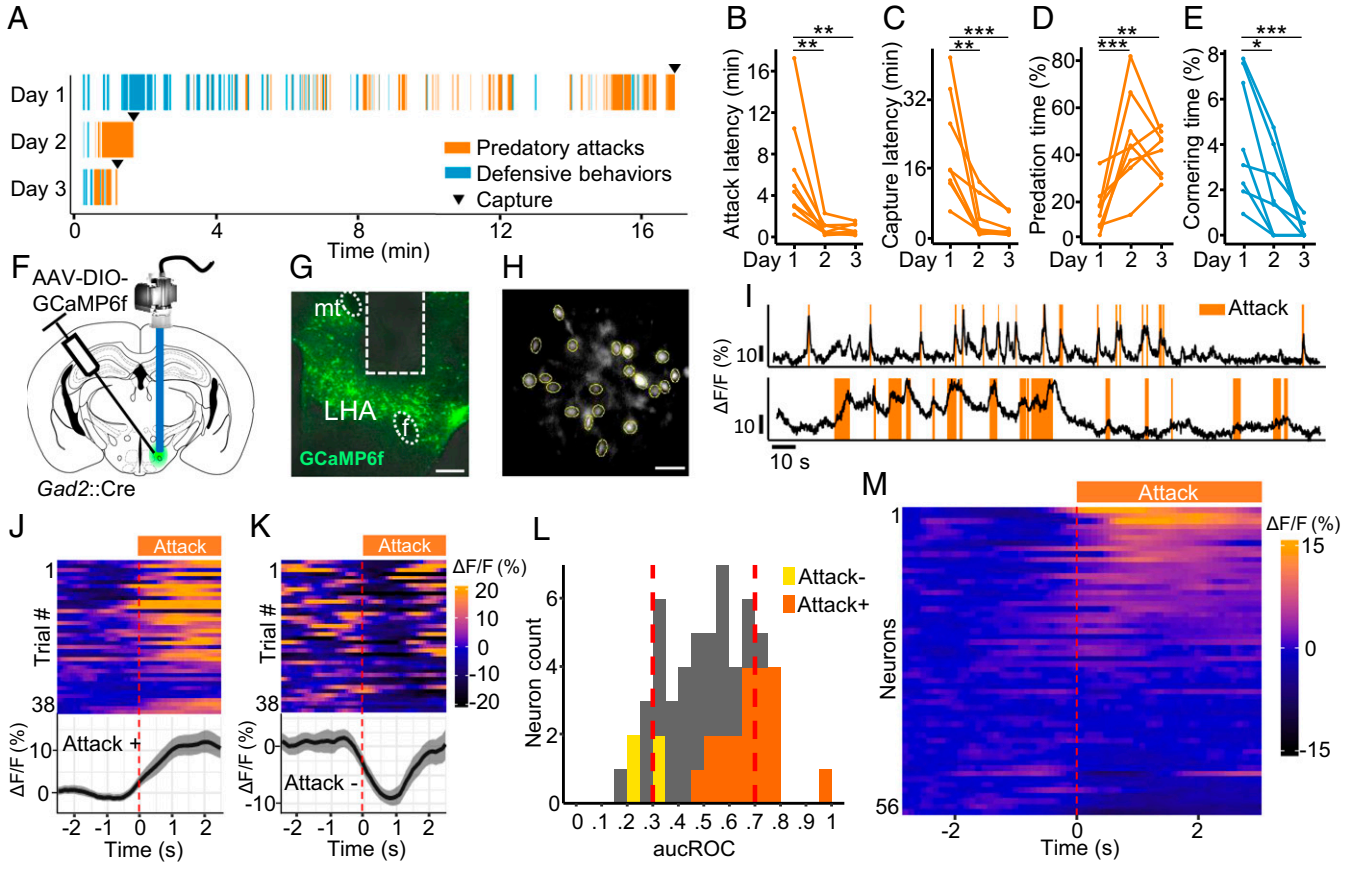

Fig. 1. LHA Gad2+ neurons are recruited during predatory attack. (*A*) Raster plot illustrating the occurrence of aggressive and defensive behaviors of a representative mouse over 3 consecutive days of predation training. (*B*–*E*) Quantification of defensive and predatory behavior over training days ($n = 8$). (*F*) *Gad2*+ transgenic mice were infected with a Cre-dependent GCaMP6f-expressing virus, and the activity of LHA *Gad2*+ neurons was recorded in living animals using microendoscopy ($n = 5$). (*G*) Representative section showing GRIN lens placement (*mt*: mamillary tract, *F*: fornix). (Scale bar, 250 μm.) (*H*) Representative postprocessed calcium imaging field of view with ROIs indicated by yellow circles. (Scale bar, 50 μm.) (*I*) Activity trace (ΔF/F) of two representative cells recruited during predatory attack. (*J*) Response of a cell whose activity was significantly increased following attack onset (Attack+, top: activity heat map where each line corresponds to a single attack event aligned to onset, bottom: average activity trace of 38 attack events aligned to attack onset; ΔF/F ± SEM). (*K*) Response of a cell whose activity was significantly decreased following attack onset (Attack−, top: activity heat map where each line corresponds to a single attack event, bottom: average activity trace of 38 flight events aligned to attack onset). (*L*) Histogram of auROC values for all cells (56 cells, $n = 5$). ROI fluorescence per frame is used to classify attack versus nonattack periods. Vertical dashed lines indicate high (0.7) and low (0.3) cutoff (Attack+: dark orange, Attack−: light orange). (*M*) Peri-attack activity heatmap for all cells aligned to attack onset. Cells are ranked by activity increase at attack onset ($n = 5$, Bonferroni post hoc test: $^*P < 0.05$, $^{**}P < 0.01$, $^{***}P < 0.001$).

and its evolution over training days allowed us to investigate the recruitment of neural circuits involving the balance between approach and defense toward prey during hunting. We chose to investigate male mice as they would allow us to directly compare the neural circuit basis of both predatory and social aggressive behaviors, the latter of which are readily elicited only in male mice.

Lateral Hypothalamus Neurons Encode Hunting. Because of the previous report that *Gad2*+ neurons were linked to physical activity, but not feeding (23), we investigated whether this subclass of GABAergic neuron is recruited during predation. For long-term monitoring of neural activity, male mice were surgically implanted with a gradient-index (GRIN) lens cannula adapted to fit a head-mounted miniature fluorescent microscope following viral delivery of the genetically encoded calcium sensor GCaMP6f (AAV-*Ef1a*::DIO-GCaMP6f) in the LHA (Fig. 1 *F–H*, *SI Appendix*, Fig. S1*E*, and Movie S2). We expressed the calcium sensor in *Gad2*+ neurons using a Cre-dependent virus delivered to *Gad2*::Cre driver mice. Following 5 to 9 d of training, surgically treated mice showed robust and repeated hunting episodes with very few defensive responses to prey. A significant number of recorded neurons showed activity patterns that correlated with predatory attack of prey across hunting episodes (Fig. 1*I*). To identify neurons with significant hunting-correlated activity, calcium activity signals surrounding the initiation of predatory attacks were superimposed across episodes and statistically assessed (n = 5 mice, 12 to 38 episodes). A subset of neurons showed a significant positive (20/56, 36%) or negative (4/56, 7%) correlation with attack initiation (Fig. 1 *J*, *K*, and *M*). The significance of these correlations was confirmed by a bootstrap analysis in which we replaced the attack events by randomized events (*SI Appendix*, Fig. S1*F*). Subsets of neurons showed a global decrease (6/56, 11%) or increase (10/56, 17%, corresponding to <0.3 and >0.7 area under the receiver operator characteristic [auROC] score, respectively) in activity that was greater during episodes of hunting relative to other behaviors as assessed by analysis of receiver operator characteristic (ROC) curves (Fig. 1*L*). As expected, neurons showing increased activity to the onset of predation also tended to show increased responses during hunting episodes in the ROC analyses (Fig. 1*L*). These observations confirm that predatory chasing and attack behaviors recruit neural activity in LHA *Gad2*+ neurons.

Lateral Hypothalamus Gad2+ Neurons Are Necessary and Sufficient for Hunting. To determine whether activity in *Gad2*+ neurons in LHA is necessary and sufficient for hunting behavior, we used optogenetic activation and pharmacogenetic inhibition to selectively increase and decrease neuronal activity in the presence of a cockroach. To test whether neuronal activity in LHA *Gad2*+ neurons is sufficient to increase hunting behavior, we optogenetically stimulated the LHA of untrained *Gad2*::Cre male mice that had been bilaterally infected with AAV-*Ef1a*::DIO-ChR2-EYFP virus and exposed them to a cockroach (Fig. 2 *A–C* and *SI Appendix*, Fig. S1*A*). Light stimulation in ChR2-expressing animals presented for the first time with a cockroach did not affect the initial latency to investigate the prey when compared to control animals (Fig. 2*D*). However, light stimulation was associated with a significant decrease in latency to attack the prey in ChR2-expressing versus control animals (Fig. 2*E*), and the total time spent attacking the prey was significantly increased in ChR2 animals during light stimulation epochs or when compared to controls not expressing ChR2 (Fig. 2*F* and Movie S3). Light stimulation in ChR2 animals was also associated with significantly less defensive behavior in which the animal remained in the corner of the cage facing the prey when compared to control mice (Fig. 2*G*). Finally, we noted that ChR2 animals receiving light stimulation often did not consume the prey but released it after capture and continued with predatory pursuit, consistent with the idea that LHA *Gad2*+ neurons promote the preparatory rather than consummatory phases of hunting.

To test whether neural activity in LHA *Gad2*+ neurons is necessary to promote hunting, *Gad2*::Cre male mice were bilaterally infected in the LHA with AAV-*hSyn*::DIO-hM4D-mCherry or the control virus (Fig. 2 *H* and *I* and *SI Appendix*, Fig. S2*B*), and animals were trained to hunt efficiently by daily exposure to cockroaches over 5 d. On the sixth day, animals were treated with clozapine-*N*-oxide (CNO) 1 h before testing (Fig. 2*J*). Although CNO treatment was not associated with a significant change in latency to attack prey (Fig. 2*L*), CNO treatment significantly decreased time spent attacking (Fig. 2*K*) and increased latency to capture (Fig. 2*M*) prey in hM4D-expressing animals compared to controls. Together, these findings argue for a causal role of LHA *Gad2*+ neurons in promoting hunting but potentially not feeding.

Lateral Hypothalamus Gad2+ Neurons do Not Promote Feeding or Aggression. To directly examine whether LHA *Gad2*+ neurons are involved in feeding behavior, we optogenetically activated this population when animals were given a choice between a chamber where food was available and another where it was not (Fig. 3*A*). Light stimulation of ChR2-expressing animals did not elicit increased food consumption or time spent in a food-containing chamber when compared to controls (Fig. 3 *B* and *C*). Nevertheless, we noted that stimulation of ChR2-expressing animals triggered avid biting of food pellets and both Petri dishes (Fig. 3*D*, *SI Appendix*, Fig. S2*C*, and Movie S4). These findings confirm that *Gad2*+ neurons do not promote feeding per se but that they can trigger hunting-like capture behavior even toward nonprey objects.

Next, we investigated whether stimulation of LHA *Gad2*+ neurons might increase attack against conspecifics. Male mice were subjected to the resident–intruder test of social aggression in which a subordinate BALB/c male is introduced into the cage of a singly housed experimental animal (Fig. 3*E*). Light stimulation of ChR2-expressing resident mice was not associated with an increase in attacks toward the intruder (Fig. 3*F*); we instead observed a decrease in social activity (Fig. 3*G*), suggesting that this population does not regulate aggression toward conspecifics. However, we did observe that stimulated mice occasionally chased and bit the tail of intruders, a behavior we did not see in stimulated control animals.

These findings suggest that stimulation of LHA *Gad2*+ neurons is able to elicit predation-like behaviors (e.g., chasing, biting) toward inanimate objects. To test this hypothesis, we examined whether ChR2 stimulation of LHA *Gad2*+ neurons could drive predatory attack against a prey-like robot (Fig. 3*H*). Light stimulation of ChR2 expressed in LHA *Gad2*+ neurons was associated with pursuit and attack of the robot, a behavior not observed in control animals (Fig. 3*I*). Importantly, control animals showed a much higher level of defensive behaviors toward the artificial prey than toward a natural prey, reinforcing the conclusion that stimulation of LHA *Gad2*+ neurons is able to overcome defensive behaviors elicited by the prey to promote pursuit (Fig. 3*J*).

Finally, we tested whether optogenetic stimulation of LHA *Gad2*+ neurons had rewarding properties in the real-time place preference test (RTPP). Because evidence suggests the drive to hunt is a reinforcing mental state (16), we expected mice to seek LHA GAD2 stimulation. Light stimulation of mice expressing ChR2 in LHA *Gad2*+ neurons in one side of a two-chamber shuttle box was associated with a significant preference for the stimulated side when compared to control mice (Fig. 3 *K* and *L*). Although light stimulation of mice expressing ChR2 elicited sporadic stereotypic digging activity, a behavior not seen in the absence of light stimulation or in controls, experimental and control animals showed a similar level of locomotor activity in the stimulation chamber (*SI Appendix*, Fig. S2 *D* and *E*). These findings argue for a reinforcing effect of LHA *Gad2*+ neuron activity.

Projections from LHA to PAG Inhibit Defensive Behaviors toward Prey. We hypothesized that PAG might serve primarily to promote

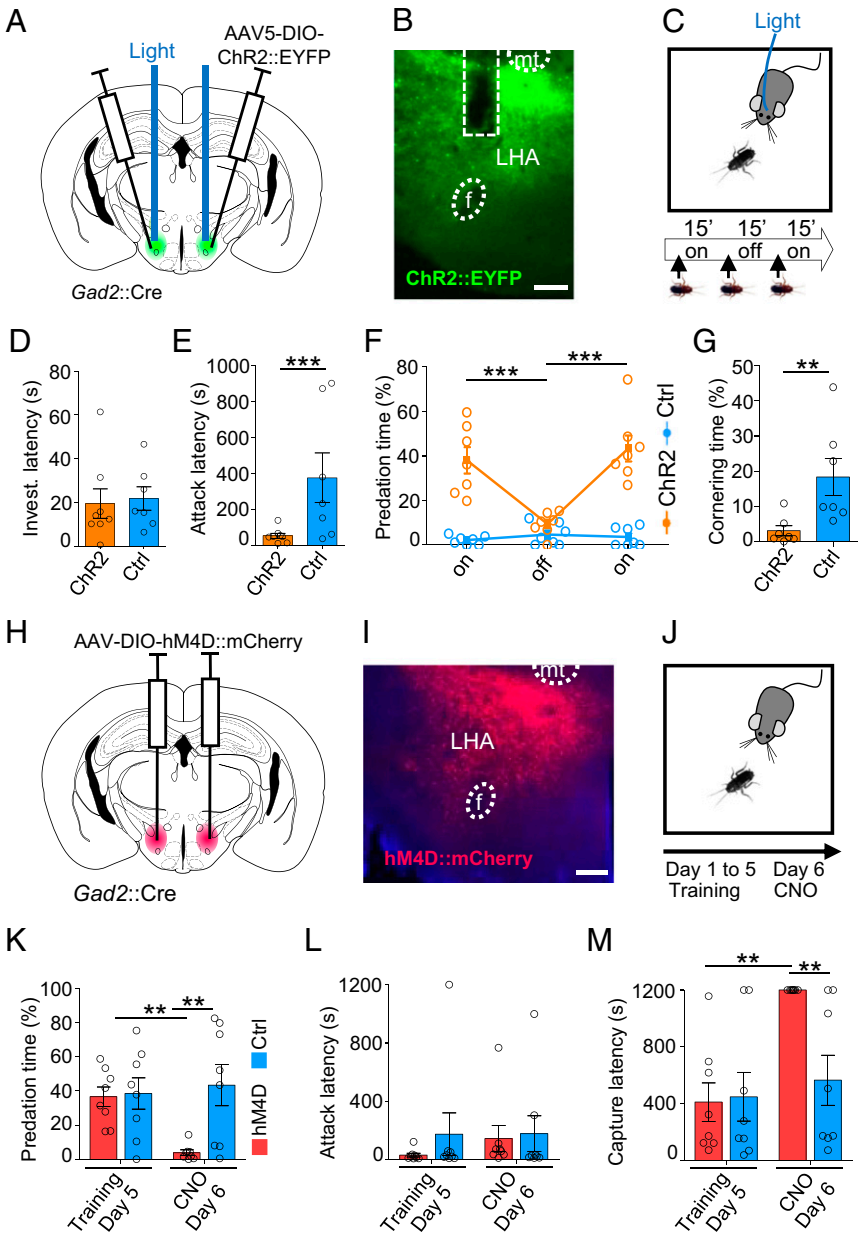

Fig. 2. LHA Gad2+ neurons promote predation. (*A*) Gad2::Cre transgenic mice were infected with a Cre-dependent ChR2-expressing or control virus bilaterally in LHA and optic fibers were bilaterally implanted in the dorsal part of the LHA. (*B*) Representative section showing ChR2 reporter expression and fiber placement in LHA. (Scale bar, 200 μm.) (*C*) Mice naïve to prey were exposed to a cockroach during two epochs of light stimulation (on, 15 min) separated by one epoch with no stimulation (off, 15 min). (*D*) Latency to begin investigation of prey (*t* test, $P = 0.47$). (*E*) Latency to attack prey (*t* test, $P < 0.0001$). (*F*) Time spent attacking the prey (ChR2: $n = 7$, $F_{(2,22)} = 13.6$, $P = 0.0001$). (*G*) Time spent cornering during first stimulation epoch (ChR2: $n = 7$, *t* test, $P = 0.0065$; unless otherwise indicated, ChR2: $n = 8$, Ctrl: $n = 7$, mean ± SEM, repeated measures ANOVA—epoch × group interaction). (*H*) *Gad2*+ transgenic mice were infected with a Cre-dependent hM4D-expressing or control virus bilaterally in LHA. (*I*) Representative section showing hM4D reporter expression in LHA. (*J*) Animals underwent predation training over 5 d and were tested on the sixth day following treatment with CNO. (Scale bar, 200 μm.) (*K*) Time spent attacking on days 5 and 6 ($F_{(2,14)} = 11.46$, $P = 0.0044$). (*L*) Latency to attack on days 5 and 6 ($F_{(2,14)} = 0.27$, $P = 0.58$). *M*) Latency to capture prey on days 5 and 6 ($F_{(2,14)} = 9.83$, $P = 0.0073$; hM4D: $n = 8$, Ctrl: $n = 8$, mean ± SEM, repeated measure ANOVA—treatment × group interaction, Bonferroni post hoc test: $^*P < 0.05$, $^{**}P < 0.01$, $^{***}P < 0.001$, *mt*: mamillary tract, F: fornix).

prey avoidance and that inhibitory projections from LHA to PAG could promote hunting by suppressing defensive responses to the prey during the initial learning phase. Consistent with this hypothesis, we confirmed that LHA *Gad2*+ neurons project to lateral and ventrolateral PAG (*SI Appendix*, Fig. S3*A*). To test whether these projections have a functional role in the suppression of defensive responses to prey, we bilaterally expressed ChR2 in LHA *Gad2*+ neurons (AAV-*Ef1a*::DIO-ChR2-EYFP) and stimulated their projections in PAG target areas (Fig. 4 *A* and *B* and *SI Appendix*, Fig. S3*B*). In untrained ChR2 animals, but not in control mice, light stimulation was associated with a significant reduction in latency to attack (Fig. 4*C*). However, this effect was not associated with a decreased latency to capture compared to controls, suggesting that only part of the predatory behavioral sequence was affected (Fig. 4*D*). Consistent with a decreased latency to initiate predation, the total time spent

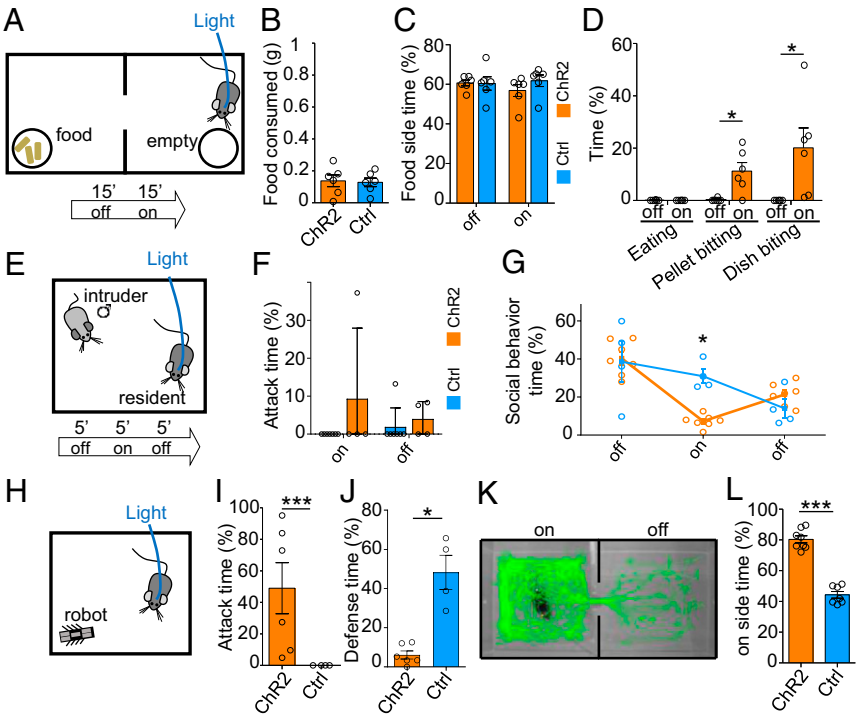

Fig. 3. LHA Gad2+ neurons do not promote feeding or aggression. (*A*) *Gad2*::Cre mice infected with a Cre-dependent ChR2-expressing or control virus in LHA and implanted with optical fibers were tested in a two-compartment apparatus with food available on one side and an empty Petri dish on the other side. Following a period without stimulation (off, 15 min) animals were stimulated with light (on, 15 min). (*B*) Food consumed ($weight_{BEFORE} - weight_{AFTER}$, *t* test, $P = 0.84$). (*C*) Time spent on food side ($F_{(2,8)} = 2.17$, $P = 0.17$). (*D*) Time spent eating or biting food pellet or Petri dish ($F_{(3,36)} = 5.59$, $P = 0.0077$; ChR2: $n = 6$, Ctrl: $n = 6$, mean ± SEM, repeated measure ANOVA—epoch × group). (*E*) To test social aggression, a subordinate mouse was introduced into the home cage of the experimental animal. (*F*) Time spent attacking the intruder ($F_{(1,18)} = 0.95$, $P = 0.34$). (*G*) Percentage of time spent performing social behavior ($F_{(2,18)} = 8.09$, $P = 0.0031$; ChR2: $n = 7$, Ctrl: $n = 4$, mean ± SEM, repeated measure ANOVA—epoch × group). (*H*) The RTPP assay was used to examine the reinforcing properties of LHA *Gad2*+ neuron stimulation. Representative path tracking in stimulated (*Left*) and nonstimulated (*Right*) compartments for a ChR2-expressing mouse. (*I*) Time spent on the stimulation side of the RTPP apparatus (*t* test $P < 0.0001$; ChR2: $n = 8$, Ctrl: $n = 7$, mean ± SEM). (*J*) Predation of a prey-like moving object was examined by introducing a small mechanical robot into the cage. (*K*) Time spent attacking the robot (Mann–Whitney *U* test, $P = 0.009$). (*L*) Time spent performing defensive behaviors in the presence of the robot ($P = 0.0005$; ChR2: $n = 6$, Ctrl: $n = 4$, mean ± SEM, Bonferroni post hoc test: $*P < 0.05$, $**P < 0.01$, $***P < 0.001$).

attacking the cockroach was significantly increased in ChR2 compared to control animals. (Fig. 4*E*). Moreover, defensive responses to the cockroach as measured by cornering behavior were significantly reduced in ChR2 mice compared to controls (Fig. 4*F*). A similar decrease in defensive behaviors was seen toward the mechanical robot. Notably, in some cases, stimulated animals proceeded to attack the robot, something that was only rarely observed in unstimulated or control animals (Fig. 4*G*). These findings support a role for *Gad2*+ LHA–PAG projections in promoting predation and suggest that this occurs at least in part via a reduction in defensive response to prey.

PAG Neurons Encode Defensive Behaviors Elicited during Predation. To test the hypothesis that PAG neurons might primarily encode defensive response during predation, we performed in vivo calcium microendoscopy in lPAG of mice exposed repeatedly to a cockroach. GCaMP6f (AAV-*hSyn*::GCaMP6f) was expressed in l/vlPAG, and animals were surgically implanted with a microendoscope above lPAG and exposed over several days to a cockroach (Fig. 4 *H* and *I* and *SI Appendix*, Fig. S3*C*). On the first day of training, when mice exhibited frequent flights from the prey, a significant number of neurons showed activity patterns that were visibly correlated with defensive behavior (Fig. 4*J*). To identify neurons in PAG with significant behavior-correlated activity, calcium activity signals surrounding the initiation of flight episodes were superimposed and statistically assessed. A large fraction of neurons (39%, 34/88) showed a significant increase in activity time locked to the onset of flight (Flight+; Fig. 4 *K*, *N*, and *O*). A smaller proportion of neurons (11%, 10/88) showed a significant decrease in activity at the onset of flight (Flight−; Fig. 4 *L*, *N*, and *O*). The significance of these correlations was confirmed by a bootstrap analysis in which we replaced the flight events by randomized events (*SI Appendix*, Fig. S3*D*). Flights were often preceded by risk assessment behaviors oriented toward the prey, including stretched approach, sniffing, and rearing. Notably, most Flight− cells showed an increase in activity during this risk assessment period, increasing their activity up to the moment of flight onset and then returning to baseline thereafter (Fig. 4*L*). Because these units showed significant time-locked activity to the onset of risk assessment behaviors, we labeled them as assessment cells (Assessment+; Fig. 4*M*).

To understand whether PAG activity was modulated by the level of fear toward the prey, we examined the activity of neurons in animals trained to efficiently hunt prey and showing no or only very infrequent defensive behaviors (5 to 9 d of training). Under these conditions, mice showed prey pursuit and attack that were not associated with risk assessment or followed by flight. Consistent with the absence of flight behaviors, we failed to detect Flight+ cells during or following prey attack, although we did observe one unit whose activity significantly increased at attack onset (Fig. 4 *N* and *P*). Notably, we failed to detect any units whose activity was correlated with approach to prey. These observations suggest that the Assessment+ cell activity seen during

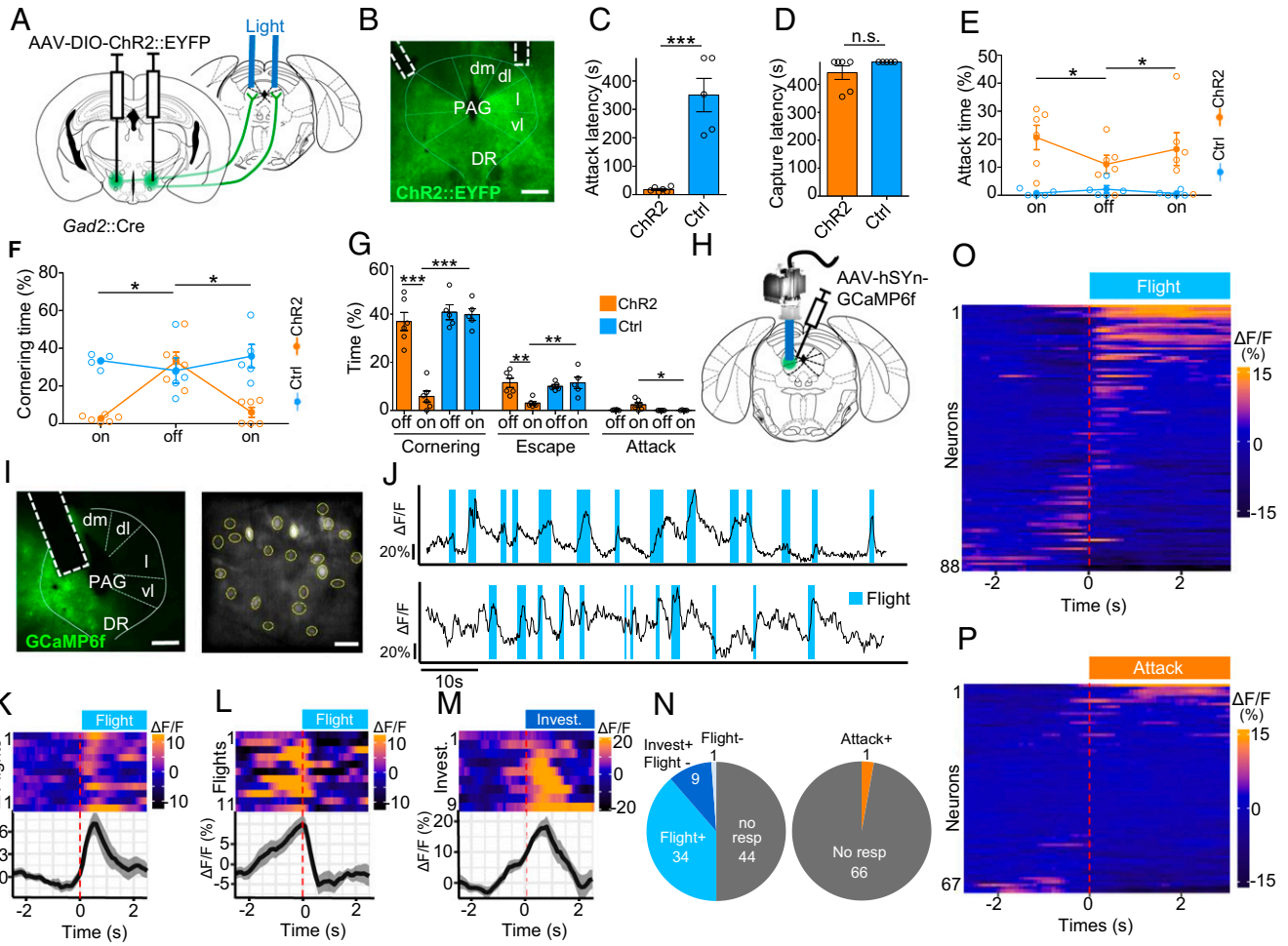

Fig. 4. LHA to PAG projections inhibit defensive response to prey. (*A*) *Gad2*::Cre mice infected with a Cre-dependent ChR2-expressing or control virus in LHA and implanted with optical fibers over lPAG were tested for predatory hunting. On the first day of testing, animals were subjected to a period without stimulation (off, 8 min) followed by light stimulation (on, 8 min). (*B*) Representative section showing ChR2 reporter expression and fiber placement (*dm*: dorsomedial, *dl*: dorosolateral, *l*: lateral, *vl*: ventrolateral, *DR*: dorsal raphe). (Scale bar, 400 μm.) (*C*) Latency to attack prey (*t* test, $P = 0.0001$). (*D*) Latency to capture prey (Mann–Whitney *U* test, $P = 0.56$). (*E*) Time spent attacking prey ($F_{(3,18)} = 4.06$, $P = 0.035$). (*F*) Time spent cornering ($F_{(3,16)} = 15.6$, $P = 0.0002$; ChR2: $n = 6$, Ctrl: $n = 5$, mean ± SEM, repeated measure ANOVA—epoch × group). In a separate group of animals, LHA to PAG projection activation was performed in mice presented a prey-like robot. (*G*) Time spent cornering (*Left*), escaping (*Center*), and attacking (*Right*) in the presence of a mechanical robot. (*H*) Mice were infected with a GCaMP6f-expressing virus, and the activity of lPAG neurons was recorded in living animals using a microendoscopy ($n = 5$). (*I*) Representative section with (*Left*) GRIN lens placement and (*Right*) postprocessed field of view. (Scale bars, *Left*, 500 μm, *Right*, 50 μm.) (*J*) Activity trace (ΔF/F) of two representative neurons recruited during flight. (*K*) Response of a neuron that significantly increased its activity at flight onset (Flight+). Each line of the heat map (*Top*) corresponds to a single attack event aligned to attack onset. Traces of neuron activity averaged across 11 flight events (*Bottom*) aligned to attack onset (ΔF/F, mean ± SEM). Response of a neuron that decreased activity at flight onset (Flight−) (*L*) or increased activity at investigation onset (Assessment+) (*M*). (*Top*) Each line corresponds to a single attack event and (*Bottom*) average responses across 38 flight events. (*N*) Distribution of neurons significantly increasing (Flight+, Assessment+) or decreasing (Flight−, Assessment−) activity at flight and investigation onset. (*O*) Distribution of neurons significantly increasing (Attack+) and decreasing (Attack−) activity at attack onset recorded in animals following successful training to hunt. Heatmap of average peri-flight neuron activity aligned to flight onset for all neurons recorded in naïve ($n = 5$) (*O*) or trained ($n = 4$) (*P*) mice. (Bonferroni post hoc test: $^*P < 0.05$, $^{**}P < 0.01$, $^{***}P < 0.001$).

approach to prey in untrained animals is not linked to prey approach or predation, per se, but rather may encode prey-associated features that are attenuated during repeated exposure or training. These data are consistent with the hypothesis that neurons in lPAG encode defensive rather than predatory behavior.

Discussion

Our data show that neural activity in a genetically defined subset of GABAergic neurons (*Gad2*+) in the LHA is necessary and sufficient to promote hunting behavior, including both prey pursuit and attack in male mice. Importantly, LHA *Gad2*+ neuron stimulation did not promote the consumption of stationary food, suggesting that this population specifically drives prey pursuit (Fig. 3 *B* and *D*). These data contrast with earlier studies which found that LHA GABAergic neurons stimulation could trigger feeding (17, 19, 20). This discrepancy may in part be explained by the observation that the *Gad2*::Cre driver line is expressed in partially nonoverlapping neural populations in LHA compared to the *Vgat*::Cre line used in these studies (23). We note that earlier studies had reported that stimulation of *Gad2*+ neurons did not elicit feeding but rather a general increase in physical activity (23). In light of our data, we interpret this increased activity as a latent predatory impulse observed in the absence of prey. Alternatively, the discrepancy may be linked to the hedonic value of prey that

may arise from a combination of chemosensory and movement cues essential to trigger predation (2, 24, 25). In this case, *Gad2*+ neurons would be selectively involved in increasing the drive to seek prey because of its rewarding nature while not affecting food seeking because it depends primarily on hunger. However, we don't favor this interpretation because stimulation of *Gad2*+ neurons elicited attack also against nonprey objects (Fig. 3*D*). It remains to be determined whether *Gad2*+ neuron activity might be more responsive to highly appetitive foods or under food deprivation, conditions which were not explored in our study.

Earlier work has shown that LHA GABAergic neurons can promote a variety of approach behaviors in addition to hunting and feeding, including social investigation and aggression, and unifying theories of LHA function point to a more general role in supporting the vigor of positively reinforced seeking behaviors (15, 30). However, although stimulation of *Gad2*+ neurons in our study triggered predatory behavior against inanimate objects, it did not increase in a similar way social aggression in the resident–intruder assay (Fig. 3*G*). Thus, our finding that *Gad2*+ stimulation promoted attack toward prey and robot, but not toward a social opponent, highlights the distinction between social and predatory aggression. While social defensive aggression has been associated with an aversive internal state, predation has been associated to a rewarding state. This distinction is consistent with the proposed role for LHA in supporting the appetitive drive involved in the preparatory phase of predation (16) and is consistent with our finding that stimulation of *Gad2*+ neurons was reinforcing in the RTPP assay (Fig. 3*L*).

Predatory and defensive abilities coevolve in predator and prey in response to each other in a process referred to as an evolutionary "arms race." As a result, predation involves risks even for apex predators that often show defensive behaviors toward prey (31). Our findings suggest that the balance between predation and defense depends in part on the cross-inhibition between LHA neurons that promote the motivation to hunt and lPAG neurons that promote defensive responses to prey. Stimulation of LHA neurons during the initial trials could overcome defensive responses to the prey and increase hunting (Fig. 2 *F* and *G*), and this could be mimicked by stimulation of their projections to lPAG (Fig. 4 *E* and *F*). The role of PAG in defense was supported by our discovery of two distinct neuronal populations in lPAG whose activity was time locked with prey assessment and flight, respectively (Fig. 4 *K*–*M*). The existence of neurons encoding both approach and defense appears contradictory with a role for lPAG in promoting flight. However, similar populations have been observed in dorsomedial PAG during approach–avoidance behavior to a natural predator (32, 33), and we hypothesize that these populations coordinate defensive responses to prey by promoting risk assessment and triggering escape. It remains to be explored whether Assessment+ and Flight+ neurons in lPAG respond to and mediate defensive response to diverse innate threats, for example, predators versus prey threats, as this area has been shown to elicit active defensive responses in mice (26, 34–36). It will also be important to assess the relative contributions to other brain regions that have been implicated in hunting, including projections from the central nucleus of the amygdala (3, 4) and the medial preotic area (3, 4) to the vlPAG. Moreover, Gad2+ LHA neurons project to several other midbrain regions that may contribute to defense.

Our study focused on predatory behaviors in sexually inexperienced male mice. Although we observed that male and female mice show a similar switch from defensive to predatory behaviors when exposed to cockroaches, further work to understand potential differences in the neural control of predation between sexes is merited. In particular, sexually inexperienced males have been shown to carry out infanticide, a type of within-species predatory behavior not seen in females or sexually experienced males. The rhomboid nucleus has been shown to be essential for infanticide in mice (37) and is known to project to LHA. Thus, female sex and sexual experience in males could exert its antagonistic effect on within-species predation via LHA afferents.

In conclusion, our data are consistent with a model in which inhibitory afferents to lPAG directly suppress the firing of neurons that promote risk assessment and flight and thereby allow fearless predation. This model allows us to propose a role for lPAG as a brake rather than as an accelerator for predation. It follows that lPAG may function more widely to antagonize seeking behaviors driven by LHA or other upstream structures. Under such a model, a gradual increase in inhibitory inputs to lPAG over the course of repeated exposure to prey, including those from LHA, gradually suppresses lPAG activity and lowers defensive responses to prey. An alternative hypothesis is that inhibitory afferents to lPAG promote predation by suppressing activity in lPAG that tonically antagonizes approach behavior. However, although we cannot rule out that low levels of tonic activity escaped detection in our in vivo calcium imaging experiments, we do not favor this hypothesis as we did not observe cells in lPAG whose activity was suppressed during prey pursuit or attack. Our findings may be relevant to understanding several recent studies examining the role of PAG afferents in predation. Based on our data, we hypothesize that GABAergic inputs from CeA and ZI that promote hunting may do so by blocking defensive behaviors elicited by prey rather than by promoting predation directly. More work aimed at manipulating and recording these circuits in animals during the entire span of predatory learning will be required to test whether our findings generalize across lPAG afferent circuits.

Materials and Methods

Animals and Behavioral Apparatus. All experimental procedures involving the use of animals were carried out in accordance with European Union (EU) Directive 2010/63/EU and under the approval of the European Molecular Biology Laboratory (EMBL) Animal Use Committee and Italian Ministry of Health License 541/2015-PR to C.G. Animals were singly housed in temperature- and humidity-controlled cages with ad libitum access to food and water under a 12 h/12 h light–dark cycle. All behavioral experiments were carried out in male C57BL/6J mice aged 4 to 8 mo and bred at EMBL. Transgenic mice were heterozygous for *Gad2*::Cre [Gad2$^{tm2(cre)Zjh}$ (38)]. All tested animals were singly housed either from the date of surgery or from 1 wk before testing for animals not undergoing surgery and the pharmacogenetic experiments. Subordinate mice in the resident–intruder test were BALB/c males mice aged 7 wk old and bred at EMBL. Prey were adult female Turkestan cockroaches (*B. Lateralis*, 2 to 3 cm) purchased from commercial pet supply distributors in Italy and propagated at EMBL.

Surgical Procedures. Mice were anesthetized with 3% isoflurane (Provet) and subsequently head fixed in a stereotaxic frame (Kopf) with body temperature maintained at 36 ± 2 °C and anesthesia sustained with 1 to 2% isoflurane and oxygen. The skull was exposed, cleaned with hydrogen peroxide (0.3% in water), and leveled. Craniotomy was performed with a handheld drill, and, when needed, extra holes were drilled to fit two or three implant-stabilizing miniature screws (RWD). For optogenetic activation experiments, 0.2 to 0.3 μl AAV5-*Ef1a*::DIO-ChR2(E123T/T159C)-EYFP or AAV5-*Ef1a*::DIO-EYFP (University of North Carolina at Chapel Hill [UNC] Vector Core and Addgene, respectively) virus was injected bilaterally in the LHA via a pulled glass capillary attached to a pneumatic injection system [anteroposterior (AP) −1.9, medio-lateral (ML) 0.95, dorso-ventral (DV) 5.5 from Bregma]. Optic fibers were implanted bilaterally in the dorsal part of the LHA (0.66 numerical aperture [NA], 200 μm, Prizmatix; 230/1,250 μm internal/external diameter ceramic ferrule, Thorlabs). Implants were attached to the skull using dental cement (Duralay) and secured with screws fixed to the skull. One of the two fibers was implanted with an angle due to space constraints and to prevent the bilateral lesion of overlying brain structures (LHA: 15° inclination, AP −1.9, ML 1.6, DV 5.5; AP −1.9, ML 0.95, DV 5.5; PAG: 26° inclination, AP −4.4, ML 1.8, DV 2.7; AP: −4.4, ML 0.5, DV 2.2). For in vivo calcium endoscopy, 0.2 to 0.3 μl AAV5-*hSyn*::DIO-GCaMP6f virus (Penn Vector Core) was infused in the LHA (AP −1.9, ML 0.95, DV 5.5) of *Gad2*::Cre mice, or AAV5-*hSyn*::GCaMP6f was infused in the l/vlPAG (AP −4.4, ML 0.6,

DV 2.6). Endoscope GRIN lens imaging cannulas (LHA: model E, PAG: model L, type V, Doric Lenses) were implanted in the LHA (AP −1.9, ML 0.95, DV: 5.0) and lPAG (20° inclination, AP −4.4, ML 1.6, DV 2.6) and implants were attached to the brain using dental cement (Duralay). Approximately 1 h before the end of surgery, an analgesic was administered (Carprofen 5 mg/kg). Immediately after surgery, mice were intraperitoneally (i.p.) injected with 0.4 mL saline and allowed to recover in heated cages. For 3 d, post-surgery drinking water was supplemented with paracetamol (10 mL/l). For pharmacogenetic experiments, AAV8-*hSyn*::DIO-hM4D-ires-mCherry and AAV8-*hSyn*::DIO-mCherry (UNC Vector Core and Addgene, respectively) viruses were infused in the LHA (AP −1.9, ML 0.95, DV 5.5).

Hunting Test. The cage cover holding food and water was removed and replaced with a filter paper lid before mice were tested for predation in their home cage. An adult cockroach was placed in the cage until capture occurred. If prey was captured in less than 4 min, the cockroach was replaced. Cockroaches were removed before the mouse could progress to eat the prey, although it was not always possible to prevent consumption. Behaviors were recorded for scoring using cameras placed on the side and/or top of the cage. Animals used for the female and male comparison received saline injections (i.p.) 1 h prior to testing.

In Vivo Calcium Microendoscopy. Expression of GCaMP6f was allowed to proceed for 4 to 6 wk following infection. Mice were habituated over 3 d to the testing cage and the procedure of microscope (Doric Lenses) plugging before testing commenced. For neural recording during predatory attacks, mice were trained for 5 to 9 d by daily exposure to three cockroaches. During each test day, several recording sessions lasting 2 to 15 min were carried out. A built-in Doric system transistor–transistor logic output signal that activated a light-emitting diode (LED) visible in the behavioral camera field of view was used to time stamp the behavioral videos and correlate them to the calcium imaging recordings. LED intensity for GCaMP6f stimulation was adapted to each implant (15 to 60% max power, 10 Hz). Side and/or top cameras were used to track behavior. For LHA recordings, data were successfully collected from nine out of 18 animals that underwent surgery. Only animals with >nine distinguishable neurons and histologically confirmed fiber placement were included in the analysis (5/9). For PAG recordings, data were successfully collected from 11 out of 18 animals (5/11 with >nine neurons and correct fiber placement).

Optogenetic Stimulation. Viral expression was allowed to continue for at least 2 wk (4 wk for projection activation). Mice were habituated over 3 d to handling and optic fiber plugging before testing commenced. Optical stimulation was performed with double LED modules (465 nm, Plexbright, Plexon) directly attached to a rotary joint and connected to the implant via a patch cable (1 m, 0.66 NA, Plexbright High Performance, Plexon). Power at the tip of the implanted fiber was verified before surgery with an optical power meter (Thorlabs). Stimulation trains were generated using V2.2 Radiant software (Plexon; LHA: 20 Hz, 10 ms, 13 to 17 mW; PAG: 20 Hz, 20 ms, 13 to 17 mW). For the hunting test, the animal had no prior experience with prey, and the initiation of stimulation was concomitant with presentation of the cockroach. For technical reasons, two ChR2-expressing animals could be analyzed for only the first 15′ stimulation epochs. For the feeding test, the mouse was placed in a two-compartment Plexiglas cage (25 × 50 cm). The mouse was plugged 10 min before being placed in the apparatus containing two Petri dishes, one filled with food pellets and the other empty placed in each compartment, respectively. For the resident–intruder test, a male BALB/c intruder (6 to 7 wk old) was placed in the home cage of the tested animal. For the RTPP assay, animals were plugged 10 min before being placed in a two-chamber apparatus. For the robot experiments, a Hexbug Nano toy device was used (4 cm long, 2 cm wide, 1.5 cm high; 12 vibrating rubber legs).

Pharmacogenetic Inhibition. To ensure inhibition of a wide distribution of LHA neurons, we opted for a pharmacogenetic neural inhibition approach. Virus expression was allowed to proceed for 3 wk. Testing took place in the home cage following training during which mice were allowed to hunt and consume two cockroaches per day for 5 consecutive days. An hour before each training session, animals received an i.p. saline injection. Behavior was scored on the last training day as baseline. On the testing day, all animals received CNO (3 mg/kg, 0.9% saline, i.p.) 1 h before exposure to prey.

Behavioral Data Analysis. Behavioral scoring was performed manually using Solomon Coder software at 100 or 200 ms bin frame rate with the experimenter blind to calcium trace or experimental group. Behaviors were defined as the following—*flight*: rapid and stereotyped running away from prey or robot; *cornering*: immobile in the cage corner facing prey (frequently observed following *flight*); *jump escape*: repeated jumping against the cage walls (frequently observed when prey approached the cornered mouse); *attack*: aggressive behavior toward the prey or robot using forepaws or mouth (usually coinciding with a horizontal straightened tail), and the prey is not immobilized; *capture*: prey immobilization with both forepaws and biting; *investigation*: sniffing environment, often while rearing; *social behavior*: anogenital and facial sniffing and back biting (tail biting was not considered social behavior); *eating*: grabbing food using both forepaws and/or mouth chewing; *food pellet biting*: biting without grabbing or chewing; *digging*: stereotypic coordinated forepaw movements often occurring at the base of the cage walls; and *locomotor activity*: the time mice spend traveling in the cage. Time spent in each chamber in the RTPP assay was determine by automatic body tracking with Viewer software (Biobserve). All behavioral videos from a single experiment were scored by the same experimenter. The intra and interexperimenter reliability was estimated over 20 min of concatenated videos scored for attack, flight, and cornering by three experimenters. The complete time series vectors of behavioral scoring were compared using Fleiss' kappa. Intraexperimenter reliability kappa ranges were 0.917 to 0.964 for attacks, 0.826 to 1.00 for flights, and 0.865 to 1.00 for cornering. Interexperimenter reliability kappa were 0.901 for attacks, 0.792 for flights, and 0.828 for cornering.

Histology. Animals were anesthetized with Avertin (2.5%, i.p.) and transcardially perfused with phosphate-buffered saline (PBS) followed by 4% paraformaldehyde (PFA; Sigma) in 0.1 M phosphate buffer solution. The brain was then extracted from the skull, postfixed in 4% PFA for 24 h at 4 °C, and sectioned (20 to 60 μm) using a vibratome (Leica VT1000 S). If necessary, sections were stored in PBS 0.01% sodium azide. For viral transgene expression or implant track position verification, sections were mounted on slides and imaged using an epifluorescence or confocal microscope.

Calcium Imaging Analysis. Image processing was performed with ImageJ/Fiji software. Videos were batch processed using a customized macro. The background of each frame was calculated using an FFT bandpass filter (lower/higher band: 100/10,000, Fiji) and subtracted from the original images frame by frame. The resulting stack was then aligned with Fiji TurboReg, and neuronal cell body–like structures showing variation in fluorescence intensity were manually identified as regions of interest (ROIs, elliptical areas). Several ROIs were designated in areas not containing any visible neurons as negative controls. The average fluorescence intensity of ROIs for each frame were extracted (F). ROIs were not tracked across days. $\Delta F/F$ ($F\text{-}F_0/F_0$) was calculated for each ROI, where F_0 was the mean fluorescence intensity of the ROI over the entire recording period. A few isolated frames (<1/1,000) appeared completely black because of technical issues, and ROIs of these frames were interpolated from adjacent frames. ROIs were included in the analysis only if they had at least one transient response, calculated as three consecutive frames during the whole recording session being at least twice the SD of the preceding 5 s. To eliminate interference between brief and adjacent behavioral events, and to account for GCaMP6f decay time, events that occurred twice within a 3 s time window were excluded. The peri-behavioral traces were centered on the intensity mean of 5 s preceding the behavior onset. Average responses for each neuron were obtained by averaging the normalized intensities across all events and smoothed using a four-point rolling mean. Statistics to identify cells responding to a given behavior were performed on the average response of at least nine trials. For ROC analyses, all frames from selected calcium imaging recording sessions were classified as "attack" or "no attack." A ROC curve was generated for each neuron by plotting the true positive and false positive rates across the distribution, and the auROC was calculated with 0.3 and 0.7 selected as thresholds for classification.

Statistical Analysis. Prism GraphPad 5 software or custom R scripts were used to generate graphs and perform statistical analyses. Unless otherwise indicated, for optogenetic and pharmacogenetic experiments, repeated measures ANOVA with Bonferroni post hoc test as well as *t* test were used. For calcium imaging, behavioral time-locked response-adjusted *t* test was used. The boot strap analyses were performed by randomly generating, for each recording, a scrambled set of events and measuring the *P* value of all the neurons from the recording.

Data Availability. All study data are included in the article and/or supporting information.

ACKNOWLEDGMENTS. We thank the EMBL Rome Laboratory Animal Facility, Genetic & Viral Engineering Facility, Microscopy Facility, and Francesca Zonfrillo, Claudia Valeri, Roberto Voci, Valerio Rossi, and Matteo Gaetani for support with animal husbandry and management, Piotr Krzywkowski and Maria Esteban Masferrer for support with calcium imaging, and Angelo Raggioli for production of viruses. The work was supported by EMBL (D.R., V.L.F., T.S., S.N., and C.T.G.), Stavros Niarchos Foundation (D.R.), and the European Research Council Advanced Grant COREFEAR (C.T.G.).

1. A. Tulogdi *et al*., Neural mechanisms of predatory aggression in rats-implications for abnormal intraspecific aggression. *Behav. Brain Res.* **283**, 108–115 (2015).
2. J. L. Hoy, I. Yavorska, M. Wehr, C. M. Niell, Vision drives accurate approach behavior during prey capture in laboratory mice. *Curr. Biol.* **26**, 3046–3052 (2016).
3. W. Han *et al*., Integrated control of predatory hunting by the central nucleus of the amygdala. *Cell* **168**, 311–324.e18 (2017).
4. S. G. Park *et al*., Medial preoptic circuit induces hunting-like actions to target objects and prey. *Nat. Neurosci.* **21**, 364–372 (2018).
5. Y. Li *et al*., Hypothalamic circuits for predation and evasion. *Neuron* **97**, 911–924.e5 (2018).
6. A. Tulogdi *et al*., Brain mechanisms involved in predatory aggression are activated in a laboratory model of violent intra-specific aggression. *Eur. J. Neurosci.* **32**, 1744–1753 (2010).
7. E. Comoli, E. R. Ribeiro-Barbosa, N. Negrão, M. Goto, N. S. Canteras, Functional mapping of the prosencephalic systems involved in organizing predatory behavior in rats. *Neuroscience* **130**, 1055–1067 (2005).
8. S. R. Mota-Ortiz *et al*., The periaqueductal gray as a critical site to mediate reward seeking during predatory hunting. *Behav. Brain Res.* **226**, 32–40 (2012).
9. M. Wasman, J. P. Flynn, Directed attack elicited from hypothalamus. *Arch. Neurol.* **6**, 220–227 (1962).
10. A. Siegel, J. P. Flynn, Differential effects of electrical stimulation and lesions of the hippocampus and adjacent regions upon attack behavior in cats. *Brain Res.* **7**, 252–267 (1968).
11. J. Panksepp, Aggression elicited by electrical stimulation of the hypothalamus in albino rats. *Physiol. Behav.* **6**, 321–329 (1971).
12. C. H. Woodworth, Attack elicited in rats by electrical stimulation of the lateral hypothalamus. *Physiol. Behav.* **6**, 345–353 (1971).
13. R. J. Bandler, Predatory behavior in the cat elicited by lower brain stem and hypothalamic stimulation: A comparison. *Brain Behav. Evol.* **14**, 440–460 (1977).
14. A. Siegel, T. A. Roeling, T. R. Gregg, M. R. Kruk, Neuropharmacology of brain-stimulation-evoked aggression. *Neurosci. Biobehav. Rev.* **23**, 359–389 (1999).
15. G. D. Stuber, R. A. Wise, Lateral hypothalamic circuits for feeding and reward. *Nat. Neurosci.* **19**, 198–205 (2016).
16. J. Panksepp, *Affective Neuroscience: The Foundations of Human and Animal Emotions* (Oxford University Press, 2004).
17. E. H. Nieh *et al*., Decoding neural circuits that control compulsive sucrose seeking. *Cell* **160**, 528–541 (2015).
18. R. van Zessen, J. L. Phillips, E. A. Budygin, G. D. Stuber, Activation of VTA GABA neurons disrupts reward consumption. *Neuron* **73**, 1184–1194 (2012).
19. J. H. Jennings *et al*., Visualizing hypothalamic network dynamics for appetitive and consummatory behaviors. *Cell* **160**, 516–527 (2015).
20. J. H. Jennings, G. Rizzi, A. M. Stamatakis, R. L. Ung, G. D. Stuber, The inhibitory circuit architecture of the lateral hypothalamus orchestrates feeding. *Science* **341**, 1517–1521 (2013).
21. M. Navarro *et al*., Lateral hypothalamus GABAergic neurons modulate consummatory behaviors regardless of the caloric content or biological relevance of the consumed stimuli. *Neuropsychopharmacology* **41**, 1505–1512 (2016).
22. A. Venner, C. Anaclet, R. Y. Broadhurst, C. B. Saper, P. M. Fuller, A novel population of wake-promoting GABAergic neurons in the ventral lateral hypothalamus. *Curr. Biol.* **26**, 2137–2143 (2016).
23. C. Kosse, C. Schöne, E. Bracey, D. Burdakov, Orexin-driven GAD65 network of the lateral hypothalamus sets physical activity in mice. *Proc. Natl. Acad. Sci. U.S.A.* **114**, 4525–4530 (2017).
24. C. Shang *et al*., A subcortical excitatory circuit for sensory-triggered predatory hunting in mice. *Nat. Neurosci.* **22**, 909–920 (2019).
25. Z. D. Zhao *et al*., Zona incerta GABAergic neurons integrate prey-related sensory signals and induce an appetitive drive to promote hunting. *Nat. Neurosci.* **22**, 921–932 (2019).
26. P. Tovote *et al*., Midbrain circuits for defensive behaviour. *Nature* **534**, 206–212 (2016).
27. N. Assareh, M. Sarrami, P. Carrive, G. P. McNally, The organization of defensive behavior elicited by optogenetic excitation of rat lateral or ventrolateral periaqueductal gray. *Behav. Neurosci.* **130**, 406–414 (2016).
28. C. T. Gross, N. S. Canteras, The many paths to fear. *Nat. Rev. Neurosci.* **13**, 651–658 (2012).
29. N. S. Canteras, M. Goto, Fos-like immunoreactivity in the periaqueductal gray of rats exposed to a natural predator. *Neuroreport* **10**, 413–418 (1999).
30. E. H. Nieh *et al*., Inhibitory input from the lateral hypothalamus to the ventral tegmental area disinhibits dopamine neurons and promotes behavioral activation. *Neuron* **90**, 1286–1298 (2016).
31. J. F. Eisenberg, P. Leyhausen, The phylogenesis of predatory behavior in mammals. *Z. Tierpsychol.* **30**, 59–93 (1972).
32. M. E. Masferrer, B. A. Silva, K. Nomoto, S. Q. Lima, C. T. Gross, Differential encoding of predator fear in the ventromedial hypothalamus and periaqueductal grey. *J. Neurosci.* **40**, 9283–9292 (2020).
33. H. Deng, X. Xiao, Z. Wang, Periaqueductal gray neuronal activities underlie different aspects of defensive behaviors. *J. Neurosci.* **36**, 7580–7588 (2016).
34. C. Fillinger, I. Yalcin, M. Barrot, P. Veinante, Efferents of anterior cingulate areas 24a and 24b and midcingulate areas 24a′ and 24b′ in the mouse. *Brain Struct. Funct.* **223**, 1747–1778 (2018).
35. R. Bandler, K. A. Keay, Columnar organization in the midbrain periaqueductal gray and the integration of emotional expression. *Prog. Brain Res.* **107**, 285–300 (1996).
36. R. Bandler, J. L. Price, K. A. Keay, Brain mediation of active and passive emotional coping. *Prog. Brain Res.* **122**, 333–349 (2000).
37. Y. Tsuneoka *et al*., Distinct preoptic-BST nuclei dissociate paternal and infanticidal behavior in mice. *EMBO J.* **34**, 2652–2670 (2015).
38. H. Taniguchi *et al*., A resource of Cre driver lines for genetic targeting of GABAergic neurons in cerebral cortex. *Neuron* **71**, 995–1013 (2011).